

Fundamental Limitations in Passive Time-Delay Estimation—Part II: Wide-Band Systems

EHUD WEINSTEIN, MEMBER, IEEE, AND ANTHONY J. WEISS, STUDENT MEMBER, IEEE

Abstract—This is the second part of a study which deals with the problem of passive time delay estimation. The focus here is on systems employing wide-band signals and/or arrays of very widely separated receivers. A modified (improved) version of the Ziv-Zakai lower bound (ZZLB) is used to analyze the effect of additive noise and signal ambiguities on the attainable mean-square estimation errors. When the lower bound is plotted as a function of signal-to-noise ratio (SNR), one observes two distinct threshold phenomena dividing the SNR domain into three disjointed segments. At high SNR, the lower bound coincides with the Cramér-Rao lower bound (CRLB). This is the ambiguity-free mode of operation where differential delay estimation is subject only to local errors. At moderate SNR (between the two thresholds), the lower bound exceeds the CRLB by a factor of $12(\omega_0/w)^2$ where ω_0 and w are, respectively, the center frequency and signal bandwidth. In this region, the ambiguities in the received signal phases cannot be resolved; however, a useful estimate of the differential delay can still be obtained using the received signal envelopes. At low SNR, the lower bound approaches a constant level depending only on the *a priori* search domain of the unknown delay parameter. In this region, signal observations are subject to envelope ambiguities as well, and are thus essentially useless for the delay estimation.

I. INTRODUCTION

A. Ambiguity Phenomena in Time Delay Estimation

ESTIMATION of the time difference of arrival of a noise-like random signal observed at two or more spatially separated receivers is a problem of considerable practical interest in many disciplines such as underwater acoustics, geophysics, and radio astronomy, to mention a few. Consequently, numerous procedures have been proposed for passive time-delay estimation (e.g., [1]–[7]). In most of the systems which have been analyzed, the Cramér-Rao inequality has been used to set a lower bound on the attainable mean-square estimation errors. Its use was justified by invoking a well-known theorem in statistics asserting that the maximum likelihood (ML) estimator is asymptotically unbiased, and that its error variance approaches the Cramér-Rao lower bound (CRLB) arbitrarily close for sufficiently long observation times. There remains the question: How long is “long enough”? Clearly, the observation time T must be large compared to the correlation time (inverse bandwidth) of signal and noise ($WT/2\pi \gg 1$), a condition which presents very little difficulty in practice. However,

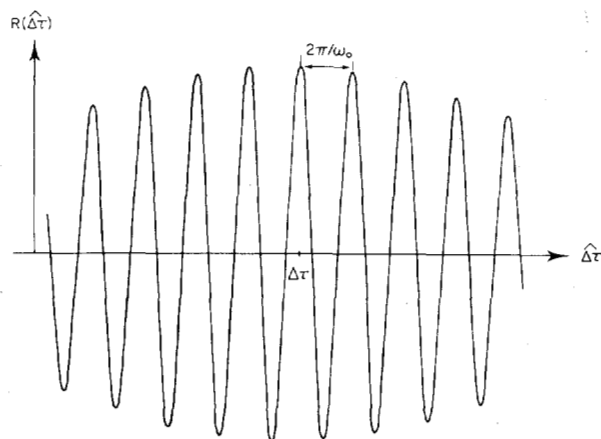


Fig. 1. Typical narrow-band signal cross correlation.

if one examines the problem more closely, one finds a second condition: the ML estimator (which approaches the CRLB asymptotically) must not be subject to ambiguities.

Perhaps the most common setting in which this difficulty occurs is in delay estimation using very narrow-band signals. Consider the extreme case of observations at only two receivers so that only one differential delay can be estimated. The ML estimate of that delay cross correlates the received signals, averages for time T , and obtains the desired delay from the peak of the cross-correlation function. In the narrow-band case, the differential delay causes essentially a phase shift between the received signals, and thus generates a formidable ambiguity problem. This is illustrated in Fig. 1. The cross-correlation output peaks at $\Delta\tau$, the true differential delay, but it is quasiperiodic with a period of $2\pi/\omega_0$ where ω_0 is the center frequency of the signal. To come close to the CRLB, one must be able to distinguish unambiguously between adjacent peaks of the correlation function. If the signal bandwidth is only a small fraction of its center frequency (i.e., $w/\omega_0 \ll 1$), adjacent peaks have very nearly equal height, and identification of the largest one will require either very large SNR or exceedingly long observation times. In many important practical situations, therefore, the attainable mean-square error (MSE) may be very drastically inferior to that predicted by the CRLB.

In [8], a new lower bound, based on a modified (improved) version of the Ziv-Zakai lower bound (ZZLB), is developed to analyze the attainable MSE in delay estimation schemes. The resulting lower bound is then applied to investigate the effect of ambiguity on delay estimation using narrow-band signals

Manuscript received August 31, 1983. This work was supported by the Naval Underwater Systems Center under Contract 00140-83-C-KA35.

E. Weinstein is with the Department of Ocean Engineering, Woods Hole Oceanographic Institution, Woods Hole, MA 02543, and with the Department of Electronic Systems, Faculty of Engineering, Tel-Aviv University, Ramat-Aviv 69978, Tel-Aviv, Israel.

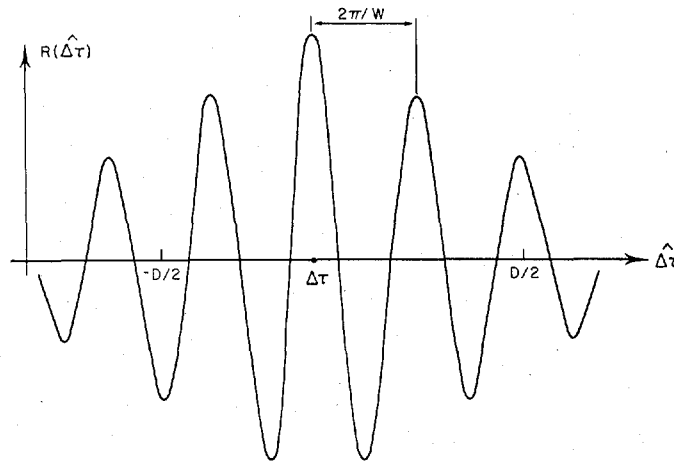


Fig. 2. Typical baseband signal cross correlation.

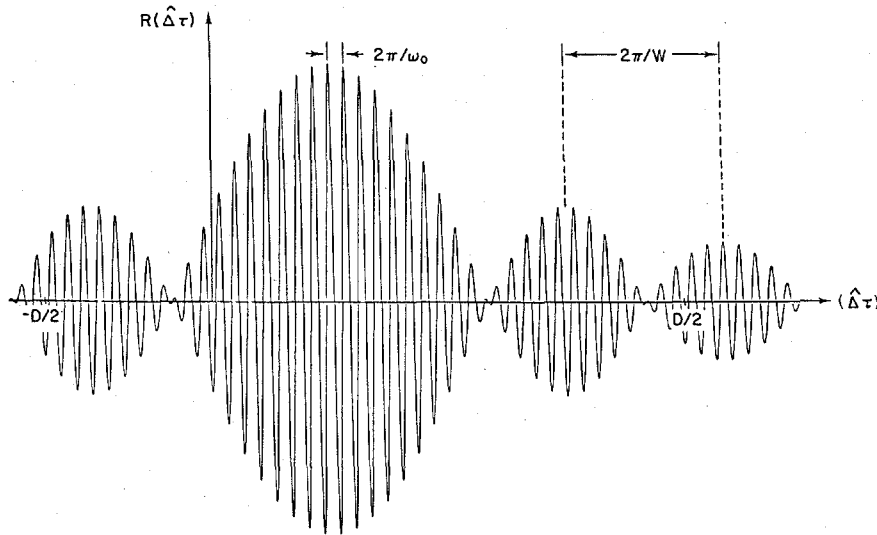


Fig. 3. Typical bandpass signal cross correlation.

[9]. When the lower bound is plotted as a function of SNR, one observes a strong threshold phenomenon. Above a critical SNR, the lower bound coincides with the CRLB. This is the ambiguity-free mode of operation. Below the threshold, the lower bound exceeds the CRLB by a large factor, indicating that in this region, differential delay estimation is subject to unresolved phase ambiguities. The point at which the threshold occurs as well as its magnitude are calculated in [9] as a function of SNR and the available WT product. Such information is of obvious practical interest since system performance predictions generally are based on the smaller error assumption (i.e., the CRLB) and may, therefore, be extrapolated incorrectly below the threshold, yielding extremely optimistic performance predictions.

In the second part of the study, we broaden the range of investigation to wide-band signals which, for the delay estimation problem, will be divided into two categories: baseband signals and bandpass signals. Both of these signal classes are subject to ambiguity and threshold phenomena. In the baseband case, a typical signal cross correlation is illustrated in Fig. 2. The cross-correlation function peaks at $\Delta\tau$, the true

differential delay, but it is an oscillatory function of the estimated delay, thus generating an ambiguity problem. In the bandpass case, the situation is even more complicated. A typical signal cross-correlation response is illustrated in Fig. 3. One observes two types of ambiguities. The more critical ambiguity problem results from the highly oscillatory nature of the phase of the observed cross correlation function. A secondary ambiguity phenomenon results from the oscillatory nature of the envelope of the cross-correlation function.

The purpose of this paper is to analyze the effect of ambiguities on the attainable MSE for these two classes of signals.

B. Problem Formulation and Assumptions

The basic system of interest here consists of a stationary source radiating a noise-like signal towards two spatially separated receivers. Each receiver also receives an additive noise component so that the actual waveforms observed at the receiver outputs are given by

$$\begin{aligned} r_1(t) &= s(t) + n_1(t) \\ r_2(t) &= s(t - \Delta) + n_2(t) \end{aligned} \quad -T/2 \leq t \leq T/2. \quad (1)$$

We shall assume that $s(t)$, $n_1(t)$, and $n_2(t)$ are sample functions from uncorrelated zero-mean Gaussian random processes with spectral densities $S(\omega)$, $N_1(\omega)$, and $N_2(\omega)$, respectively. Since we are primarily interested in the ambiguity problem in time delay estimation, implying the use of widely separated receivers, the assumption of noise incoherence from receiver to receiver is likely to be satisfied.

We shall further assume that $\Delta\tau$, the receiver-to-receiver delay, is confined to the interval

$$-D/2 \leq \Delta\tau \leq D/2. \quad (2)$$

This *a priori* domain may come about, perhaps, from the known receiver separation and the known velocity of propagation in the medium.

Finally, we shall assume that the observation time T is large compared to the correlation time (inverse bandwidth) of signal and noise, i.e., $WT/2\pi \gg 1$. This condition is very generally satisfied in problems of practical interest here.

The problem may now be stated as follows: given the data at the receiver outputs (i.e., $v_i(t)$ $i = 1, 2$), characterize the minimum MSE estimate of the delay parameter. Our approach is to set a lower bound on the attainable MSE using the modified ZZLB. This approach is completely independent from the actual estimation method. However, in [10] it is shown that for a sufficiently large WT product, the cross-correlator performance comes close to the lower bound below as well as above the threshold. These results establish the modified ZZLB as an extremely tight lower bound for problems of this type, while demonstrating that the cross correlator is a nearly optimal instrumentation in both the small and large error regimes.

C. The Modified Ziv-Zakai Lower Bound

The modified ZZLB on the MSE of any estimate $\hat{\Delta\tau}$ of $\Delta\tau$ is given by [8], [9]

$$\bar{\epsilon}^2 \geq \frac{1}{D} \int_0^D x G[(D-x)P_e(x)] dx \quad (3)$$

where $\bar{\epsilon}^2$ is the MSE averaged over the *a priori* parameter domain. $G[\]$ is a nonincreasing function of x obtained by filling the valleys in the function $(D-x)P_e(x)$ (see Fig. 12). $P_e(x)$ is the minimum probability of error (achievable by the likelihood ratio test) for deciding whether the true value of the parameter is $\Delta\tau_0$ or $\Delta\tau_1$ where $\Delta\tau_1 - \Delta\tau_0 = x$. In general, a closed analytical form for $P_e(x)$ cannot be found. However, in [9, Appendix A], it has been shown that for $WT/2\pi \gg 1$, $P_e(x)$ is very closely approximated by

$$P_e(x) \approx e^{a(x) + b(x)} \phi(\sqrt{2b(x)}) \quad (4)$$

where

$$a(x) = -\frac{T}{2\pi} \int_0^\infty \ln [1 + \text{SNR}(\omega) \cdot \sin^2 \omega x/2] d\omega \quad (5)$$

$$b(x) = \frac{T}{2\pi} \int_0^\infty \frac{\text{SNR}(\omega) \sin^2 \omega x/2}{1 + \text{SNR}(\omega) \cdot \sin^2 \omega x/2} d\omega \quad (6)$$

$$\text{SNR}(\omega) = \frac{[S(\omega)/N_1(\omega)] [S(\omega)/N_2(\omega)]}{1 + S(\omega)/N_1(\omega) + S(\omega)/N_2(\omega)} \quad (7)$$

and

$$\phi(y) \triangleq \frac{1}{\sqrt{2\pi}} \int_y^\infty e^{-u^2/2} du. \quad (8)$$

We have also included Appendix A to demonstrate that the expression on the right-hand side of (4) is, in fact, a *lower bound* on $P_e(x)$. Hence, by substituting (4) into (3), the inequality sign is preserved.

It is important to observe that since (7) uses arbitrary spectral functions, the lower bound can be applied to investigate a wide class of signals. As pointed out before, the study will be separated into two parts. In Section II we consider baseband signals. Analytically, it appears to be a simpler case and should therefore be understood first. In Section III we consider bandpass signals. In that context, all the results derived in [9] concerning narrow-band signals will be included and referred to as a special case.

II. BASEBAND SYSTEMS

In this section we shall concentrate on signals whose power is distributed about zero frequency. To simplify the form of results, let us consider the following special case:

$$S(\omega) = \begin{cases} S & |\omega| \leq W/2 \\ 0 & |\omega| > W/2. \end{cases} \quad (9)$$

If we further assume that the additive noise components are spectrally flat over $[-W/2, W/2]$, then (7) assumes the simplified form

$$\text{SNR}(\omega) = \begin{cases} \text{SNR} & |\omega| \leq W/2 \\ 0 & |\omega| > W/2 \end{cases} \quad (10)$$

where

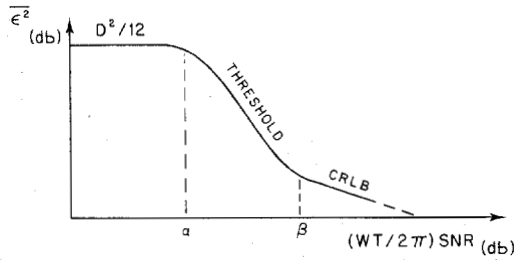
$$\text{SNR} = \frac{(S/N_1)(S/N_2)}{1 + S/N_1 + S/N_2}. \quad (11)$$

S/N_i is the in-band signal-to-noise ratio at the i th receiver output. Substitution of (10) into (5) and (6) immediately yields

$$a(x) = -\frac{T}{2\pi} \int_0^{W/2} \ln (1 + \text{SNR} \sin^2 \omega x/2) d\omega \quad (12)$$

$$b(x) = \frac{T}{2\pi} \int_0^{W/2} \frac{\text{SNR} \cdot \sin^2 \omega x/2}{1 + \text{SNR} \cdot \sin^2 \omega x/2} d\omega. \quad (13)$$

To obtain the lower bound, one must substitute (12) and (13) into (4) and (4) into (3) successively, and carry out the indicated algebraic operations. Since we are primarily interested in the ambiguity phenomenon, we shall further assume that the *a priori* search domain of the unknown delay parameter contains at least several peaks of the signal cross correlation, i.e., $WD/2\pi \gg 1$ (see Fig. 2). In that case, following some rather extensive algebra manipulations outlined in Appendix B, it is shown that the lower bound exhibits a distinct threshold effect, dividing the entire SNR domain into essentially two disjointed segments as suggested by the following

Fig. 4. Composite bound on ϵ^2 -baseband systems.

equation:

$$\epsilon^2 \geq \begin{cases} D^2/12 & (WT/2\pi) \text{ SNR} < \alpha \\ \text{threshold} & \alpha < (WT/2\pi) \text{ SNR} < \beta \\ \frac{12}{W^2} \cdot \frac{1}{(WT/2\pi) \text{ SNR}} & \beta < (WT/2\pi) \text{ SNR} \end{cases} \quad (14)$$

where, in the threshold region, the lower bound varies essentially exponentially with $(WT/2\pi)$ SNR. This result is illustrated in Fig. 4. It is interesting to observe that (14) depends on $WT/2\pi$ and SNR only through their product. This is true only if $WT/2\pi \gg 1$. The quantity $(WT/2\pi)$ SNR is usually referred to as the postintegration SNR.

α and β are the lower and upper limits of the threshold region. In the analysis carried out in Appendix B, α is defined as the point at which the lower bound is 3 dB (a factor of 2) below the $D^2/12$ performance level. It is given approximately by

$$\alpha \approx 0.92 = -0.36 \text{ dB}. \quad (15)$$

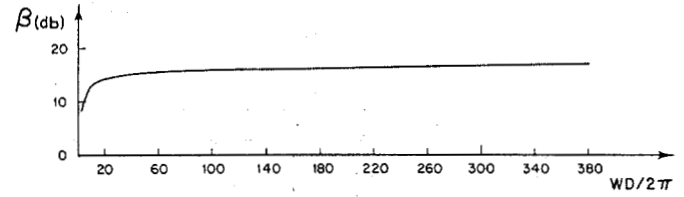
Similarly, β is defined as the point at which the lower bound is 3 dB above the performance level indicated by the third line of (14). That point is perhaps the most important factor in the composite result illustrated above, since it determines the boundary between small and large estimation errors. Analytical considerations outlined in Appendix B indicate that β is approximately the solution to the following transcendental equation:

$$(\beta/2)\phi(\sqrt{\beta/2}) = (6/WD)^2. \quad (16)$$

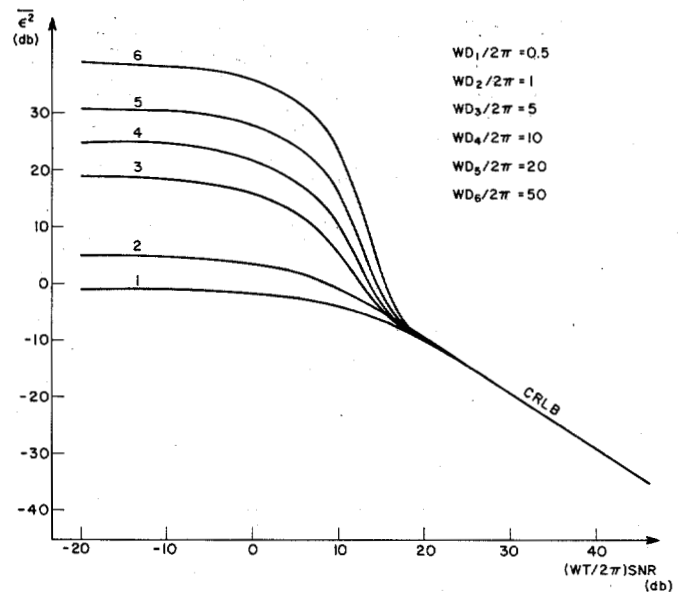
Note that (16) has two solutions. We only consider the larger one. In Fig. 5, β is plotted and tabulated as a function of $WD/2\pi$ for the convenience of the reader. Thus, in a logarithmic (dB) scale, β varies from about 13 dB for moderate WD products to about 16 dB for exceedingly large WD products.

To put these results into perspective, we first observe that a MSE of $D^2/12$ corresponds to a random variable uniformly distributed in $[-D/2, D/2]$. Such a performance level can always be achieved, regardless of signal observations. The first line in (14), therefore, reads that for a combination of $WT/2\pi$ and SNR such that their product does not exceed ~ 1 (i.e., if the postintegration SNR does not exceed ~ 0 dB), signal observations are completely dominated by noise, and thus are essentially useless for the delay estimation.

We next observe that MSE predictions based on the Cramér-Rao inequality yield the following lower bound [9, Appendix B]:



$WD/2\pi$	β	$\beta(\text{dB})$
3	7.38	8.68
10	19.33	12.86
20	25.44	14.06
60	34.98	15.44
100	39.34	15.95
140	42.17	16.25
180	44.30	16.46
220	45.91	16.62
260	47.31	16.75
300	48.60	16.87
340	49.56	16.95
380	50.53	17.04

Fig. 5. β versus $WD/2\pi$.Fig. 6. ϵ^2 versus postintegration SNR for baseband signals.

$$\epsilon^2 \geq \left[\frac{T}{2\pi} \int_0^\infty \omega^2 \text{SNR}(\omega) d\omega \right]^{-1}. \quad (17)$$

Substituting (10) into (17) and carrying out the indicated integration, one immediately obtains the third line in (14). Hence, if the postintegration SNR exceeds β , the ambiguities in the differential delay observations can essentially be resolved. By cross correlating the received signals, one obtains a differential delay estimate whose MSE is closely characterized by the CRLB.

In the derivation of (14) we have assumed that $WD/2\pi \gg 1$. This condition means that the correlation time (inverse bandwidth) of the signal is small compared to the maximum expected receiver-to-receiver delay, or that the spacing between receivers is large compared to the half-wavelength of the highest frequency component. Only in that case we are dealing with the possibility of a significant ambiguity problem. There remains the question: How are the results stated by (14) affected when this condition is not satisfied? In Fig. 6 the lower bound is generated numerically, by exact integration of

(3), and plotted as a function of the postintegration SNR (in a logarithmic (dB) scale) for different values of $WD/2\pi$. Only the upper set of curves (curves 3-6) exhibits a significant threshold phenomenon. In case $WD/2\pi < 1$, one observes a rather smooth transition from the CRLB to the $D^2/12$ asymptote. The point at which the transition occurs is given to a very good approximation by simply intersecting the first and third lines of (14).

We finally note that in the derivation of (14), it is assumed that the source signal and the additive noises are spectrally flat over the receiver frequency band. A spectrally flat signal, however, has a highly oscillatory correlation function, indicating a serious ambiguity problem. For signal spectra whose correlation function (inverse Fourier transform) is smoothly varying, the ambiguity phenomenon may not be as critical. This effect can be studied by analyzing the lower bound for various signal and noise spectra.

III. BANDPASS SYSTEMS

In this section we concentrate on signals whose power is distributed about some center frequency ω_0 . To simplify the form of results, let us consider, in complete analogy with the baseband case, the following special case:

$$S(\omega) = \begin{cases} S & |\omega \pm \omega_0| \leq W/2 \\ 0 & |\omega \pm \omega_0| > W/2. \end{cases} \quad (18)$$

We shall further assume that the additive noise components are spectrally flat over the signal frequency band so that (7) assumes the form

$$\text{SNR}(\omega) = \begin{cases} \text{SNR} & |\omega \pm \omega_0| \leq W/2 \\ 0 & |\omega \pm \omega_0| > W/2 \end{cases} \quad (19)$$

where SNR is defined in (11). Substitution of (19) into (5) and (6) immediately yields

$$a(x) = -\frac{T}{2\pi} \int_{\omega_0 - W/2}^{\omega_0 + W/2} \ln(1 + \text{SNR} \sin^2 \omega x/2) d\omega \quad (20)$$

$$b(x) = \frac{T}{2\pi} \int_{\omega_0 - W/2}^{\omega_0 + W/2} \frac{\text{SNR} \sin^2 \omega x/2}{1 + \text{SNR} \sin^2 \omega x/2} d\omega. \quad (21)$$

The lower bound is now obtained by successive substitutions of (20) and (21) into (4) and (4) into (3), and carrying out the indicated algebra operations.

Let us first assume that $W/\omega_0 \ll 1$. Since we are concerned with the joint effect of envelope and phase ambiguities on the attainable MSE (see Fig. 3), we shall further assume that $WD/2\pi \gg 1$. In this setting, therefore, we are dealing with narrow-band signals and very widely separated receivers. Following some rather extensive algebraic manipulations outlined in Appendix C, it is shown that the lower bound consists of essentially two distinct threshold effects dividing the entire SNR domain into three disjointed segments as suggested by the following equation:

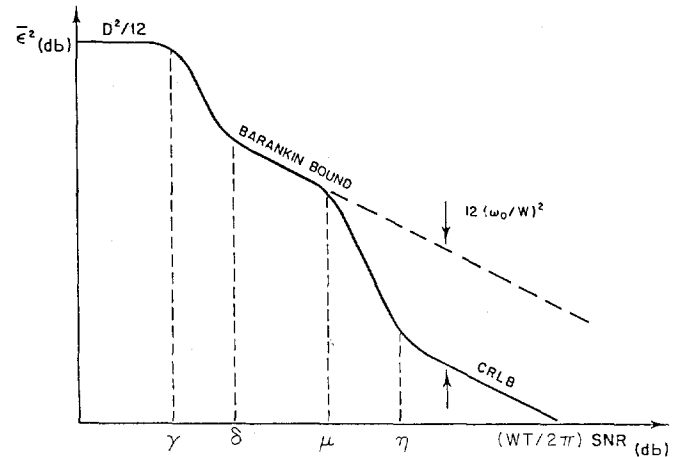


Fig. 7. Composite bound on $\bar{\epsilon}^2$ -bandpass systems.

$$\bar{\epsilon}^2 \geq \begin{cases} D^2/12 & (WT/2\pi) \text{ SNR} < \gamma \\ \text{threshold} & \gamma < (WT/2\pi) \text{ SNR} < \delta \\ \frac{6}{W^2} \frac{1}{(WT/2\pi) \text{ SNR}} & \delta < (WT/2\pi) \text{ SNR} < \mu \\ \text{threshold} & \mu < (WT/2\pi) \text{ SNR} < \eta \\ \frac{1}{2\omega_0^2} \cdot \frac{1}{(WT/2\pi) \text{ SNR}} & \eta < (WT/2\pi) \text{ SNR} \end{cases} \quad (22)$$

where, in the threshold regions, the lower bound varies essentially exponentially with $(WT/2\pi) \text{ SNR}$. Equation (22) depends on $WT/2\pi$ and SNR only through their product. This result is illustrated in Fig. 7. Analytical information concerning the various threshold points γ , δ , μ , and η will be given shortly.

To put this composite result into perspective, we observe that MSE predictions based on the Cramér-Rao inequality yield the following lower bound:

$$\bar{\epsilon}^2 \geq \frac{1}{2\omega_0^2} \frac{1}{(WT/2\pi) \text{ SNR}} \quad (23)$$

Equation (23) is obtained by substituting (19) into (17) and carrying out the indicated integration. Thus, if $(WT/2\pi) \text{ SNR} > \eta$, the CRLB coincides with the modified ZZLB. This is the ambiguity-free mode of operation.

If $\delta < (WT/2\pi) \text{ SNR} < \mu$, the lower bound exceeds the CRLB by a factor of $12(\omega_0/W)^2$. In this region, signal observations are subject to unresolved phase ambiguities. However, a useful estimate of the differential delay can still be obtained from the envelope of the cross-correlation function. Note that this segment of the lower bound coincides with MSE predictions based on a simplified version of the Barankin lower bound [11].

Finally, if $(WT/2\pi) \text{ SNR} < \gamma$, the lower bound is essentially characterized by the constant level of $D^2/12$. This is the noise-dominated region where signal observations are subject to envelope ambiguities as well, and are thus essentially useless for the delay estimation.

The 3 dB points of the more critical threshold are given, respectively, by

$$\mu = (2.76/\pi^2) (\omega_0/W)^2 \quad (24)$$

$$\eta = (6/\pi^2) (\omega_0/W)^2 [\phi^{-1}(W^2/24\omega_0^2)]^2 \quad (25)$$

where $\phi^{-1}(\cdot)$ denotes the inverse of $\phi(\cdot)$. Equations (24) and (25) depend only on ω_0/W , the ratio of center frequency to signal bandwidth. Equation (25) is of particular interest since it represents the minimum amount of postintegration SNR required to achieve the CRLB. Thus, for example, if $\omega_0/W = 10.0$ (i.e., 10 percent signal bandwidth), $\mu = 14.5$ dB and $\eta = 28.3$ dB. If $\omega_0/W = 100$ (i.e., 1 percent signal bandwidth), $\mu = 34.5$ dB and $\eta = 50.8$ dB. One further observes that the threshold region is not infinitely small, as may be interpreted from the analysis based on the Barankin lower bound [11]. For 10 percent signal bandwidth, it is a segment of $28.3 - 14.5 = 13.8$ dB. For 1 percent signal bandwidth, it is a segment of $50.8 - 34.5 = 16.3$ dB. Further discussion concerning this unavoidable threshold phenomenon and its relation to the threshold effect predicted by the Barankin lower bound is given in [9].

The 3 dB points of the secondary threshold are given, respectively, by

$$\gamma = \alpha/2 \quad (26)$$

$$\delta = \beta/2 \quad (27)$$

where α and β are defined by (15) and (16), respectively. Thus, $\gamma \approx -3.36$ dB where δ depends, to some extent, on the WD product and it varies from about 10 dB for moderate WD products to about 13 dB for exceedingly large WD products.

The derivation of (22) is based on the assumption that $W/\omega_0 \ll 1$. In that case, the lower bound exhibits two distinct threshold effects. The phase ambiguities and the envelope ambiguities occur at essentially disjointed segments of the SNR domain and are therefore, in a sense, strictly additive. As the signal bandwidth increases, the two threshold regions come close (i.e., δ converges to μ) and the two ambiguity phenomena cannot be considered separately in the SNR domain. This effect is illustrated in Figs. 8–10 where the various performance characteristics were generated for $WD/2\pi = 20$ and different values of ω_0/W by numerical integration of the exact lower bound (3). Note that $\bar{\epsilon}^2$ is normalized by $D^2/12$ so that we actually measure the relative efficiency of the attainable MSE to the *a priori* variance. The dashed lines denote the various 3 dB points calculated numerically. The sign \dagger denotes the various 3 dB points calculated using the analytical results (24)–(27). Note the close agreement between the two sets as can be observed in Figs. 8 and 9.

Narrow-Band Systems

It is not difficult to relate the composite result given by (22) to the analysis of the narrow-band systems carried out in [9]. In [9], the lower bound is derived under the assumption that the signal bandwidth is so narrow that its correlation time (inverse bandwidth) exceeds the maximum expected delay (i.e.,

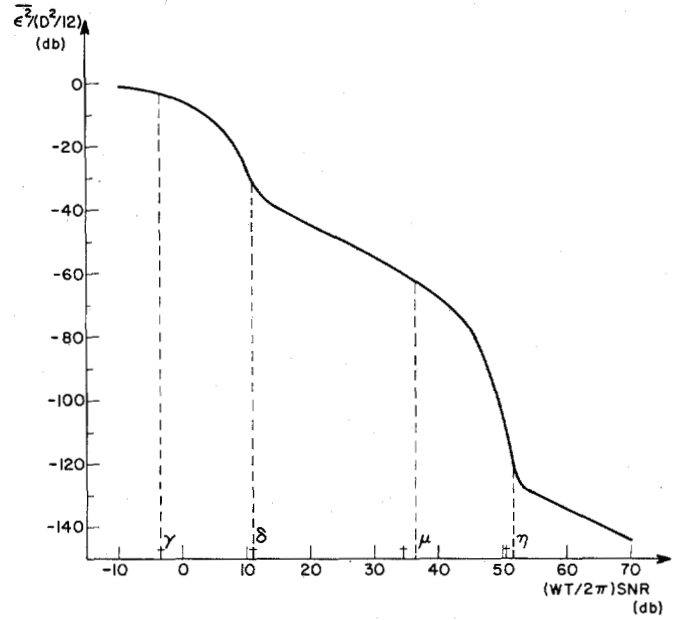


Fig. 8. Normalized $\bar{\epsilon}^2$ versus postintegration SNR for $\omega_0/W = 100$.

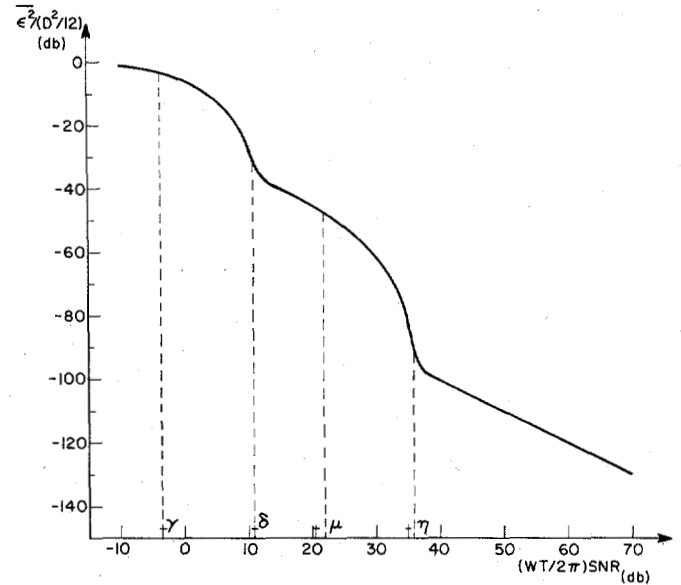
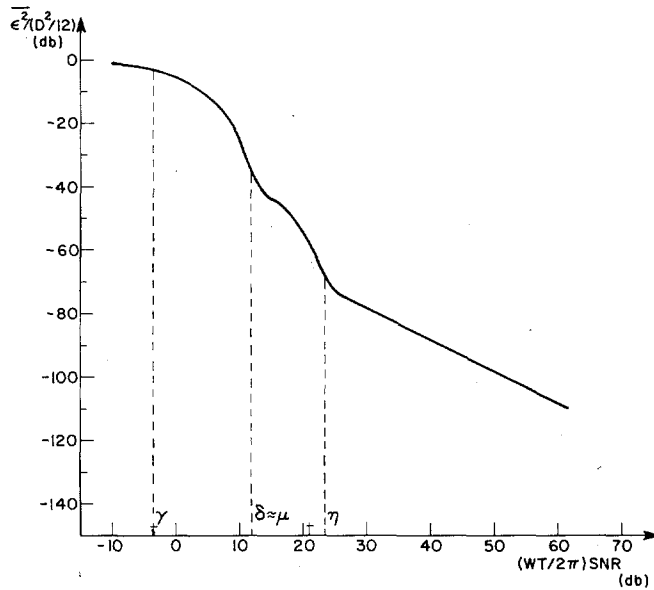
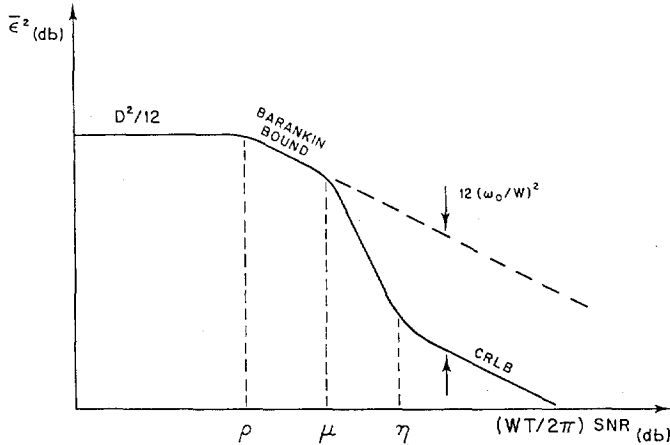


Fig. 9. Normalized $\bar{\epsilon}^2$ versus postintegration SNR for $\omega_0/W = 20$.

$WD/2\pi < 1$). The envelope-type ambiguities, therefore, are completely eliminated from consideration. Instead of having a threshold effect, there is a smooth transition from the first line of (22) to its third line as illustrated in Fig. 11. The point at which the transition occurs (denoted by ρ in the figure) is obtained by simply intersecting the two indicated lines. One finds

$$\rho = (18/\pi^2)/(WD/2\pi)^2. \quad (28)$$

With this modification, (22) reduces to the result derived in [9].

Fig. 10. Normalized $\bar{\epsilon}^2$ versus postintegration SNR for $\omega_0/W = 5$.Fig. 11. Composite bound on $\bar{\epsilon}^2$ -narrow-band systems.

IV. CONCLUSIONS

This is the second part of a study which deals with the problem of passive time delay estimation. The focus here is on systems employing wide-band signals and/or arrays of very widely separated receivers. A modified (improved) version of the ZZLB is used to analyze the effect of additive noise and signal ambiguities on the attainable mean-square estimation errors.

We first concentrated on baseband signals. The analysis is carried out in Appendix B. The lower bound is presented by (14). We observe a distinct threshold phenomenon. Above a certain postintegration SNR, the lower bound converges to the CRLB. This is the small error region where the attainable MSE varies as the first inverse power of the postintegration SNR. Below the threshold, the lower bound quickly approaches a constant level, depending only on the *a priori* search domain. In that region, signal observations are completely dominated by noise and are thus essentially useless for the delay estimation. The threshold level, which determines the boundary between small and large estimation errors, depends on *WD*, the

product of signal bandwidth by the *a priori* search domain, and it varies from about 13 dB for moderate *WD* products to about 16 dB for exceedingly large *WD* products.

Delay estimation using bandpass signals is analytically a more complicated problem. The analysis is carried out in Appendix C. The lower bound is presented by (22). Here we observe two distinct threshold effects. The location of the more critical threshold depends only on ω_0/W , the ratio of center frequency to signal bandwidth. The location of the secondary threshold depends only on the *WD* product. These threshold effects divide the entire SNR domain into essentially three disjointed segments indicating three distinct modes of operation: at high SNR the lower bound coincides with the CRLB. This is the ambiguity-free mode of operation where differential delay estimation is subject only to local errors. At moderate SNR (between the two thresholds), the lower bound exceeds the CRLB by a factor of 12 $(\omega_0/W)^2$. In that region, the ambiguities in the received signal phases cannot be resolved. However, a useful estimate of the differential delay can still be obtained from the received signal envelopes. At low SNR the lower bound approaches a constant level depending only on the *a priori* search domain. In that region, signal observations are subject to envelope ambiguities as well, and are thus essentially useless for the delay estimation.

APPENDIX A

LOWER BOUNDS ON $P_e(x)$

The binary decision problem under consideration here is given by

$$H_0: \Delta\tau = \Delta\tau_0 = a$$

$$H_1: \Delta\tau = \Delta\tau_1 = a + x. \quad (\text{A-1})$$

The log likelihood ratio test (log LRT) between H_0 and H_1 is defined by

$$l = \log \frac{p(v|H_1)}{p(v|H_0)} \quad (\text{A-2})$$

where $p(v|H_i)$ is the conditional probability density of v under H_i hypothesis, and v represents the data vector (e.g., time samples or Fourier coefficients of the received signals). Assuming that H_0 and H_1 are equally likely to occur (i.e., $P(H_0) = P(H_1) = \frac{1}{2}$), a decision rule which minimizes the probability of error compares the log LRT to a zero threshold. If $l \geq 0$, we decide on H_1 ; if $l < 0$, we decide on H_0 . Hence, the minimum attainable probability of error is given by

$$P_e(a, a+x) = \frac{1}{2} \int_0^\infty p(l|H_0) dl + \frac{1}{2} \int_{-\infty}^0 p(l|H_1) dl. \quad (\text{A-3})$$

Let $\psi_i(s)$ denote the characteristic function associated with $p(l|H_i)$. $p(l|H_i)$ and $\psi_i(s)$ are, by definition, a Fourier transform pair satisfying

$$R(l|H_0) = \frac{1}{2\pi j} \int_{c_0-j\infty}^{c_0+j\infty} \psi_0(s) e^{-sl} ds \quad (\text{A-4})$$

and

$$p(l|H_1) = \frac{1}{2\pi j} \int_{c_1-j\infty}^{c_1+j\infty} \psi_1(s) e^{-sl} ds \quad (\text{A-5})$$

where it will be shown that the integral in (A-4) can be evaluated for any c_0 in the open interval $(0, 1)$, and the integral in (A-5) can be evaluated for any c_1 in $(-1, 0)$. Substituting (A-4) and (A-5) into (A-3), one obtains

$$\begin{aligned} P_e(a, a+x) &= \frac{1}{2} \cdot \frac{1}{2\pi j} \int_{c_0-j\infty}^{c_0+j\infty} \psi_0(s) ds \int_0^\infty e^{-sl} dl \\ &\quad + \frac{1}{2} \cdot \frac{1}{2\pi j} \int_{c_1-j\infty}^{c_1+j\infty} \psi_1(s) ds \int_{-\infty}^0 e^{-sl} dl \\ &= \frac{1}{2} \cdot \frac{1}{2\pi j} \int_{c_0-j\infty}^{c_0+j\infty} [\psi_0(s)/s] ds \\ &\quad - \frac{1}{2} \cdot \frac{1}{2\pi j} \int_{c_1-j\infty}^{c_1+j\infty} [\psi_1(s)/s] ds \end{aligned} \quad (\text{A-6})$$

where the transition from the first version of (A-6) to its second version can be carried out only if $c_0 > 0$ and $c_1 < 0$. In this setting, $P_e(a, a+x)$ is expressed in terms of $\psi_i(s)$, $i = 0, 1$. Now, by definition,

$$\psi_i(s) \triangleq E\{e^{sl}|H_i\} \quad i = 0, 1 \quad (\text{A-7})$$

where $E\{\cdot\}$ denotes the statistical expectation of the bracketed quantity. Substituting (A-2) into (A-7), and observing that $l = l(\mathbf{v})$ (so that the statistical expectation operation can be performed with respect to the probability density of \mathbf{v}), one immediately obtains

$$\psi_0(s) = \int_{-\infty}^\infty [R(\mathbf{v}|H_1)]^s [p(\mathbf{v}|H_0)]^{1-s} d\mathbf{v} \quad (\text{A-8})$$

$$\psi_1(s) = \int_{-\infty}^\infty [p(\mathbf{v}|H_1)]^{1+s} [p(\mathbf{v}|H_0)]^{-s} d\mathbf{v}. \quad (\text{A-9})$$

We shall now generate the data vector \mathbf{v} by Fourier analyzing $v_k(t)$ in (1). Since signal and noise are assumed to be zero-mean Gaussian processes, and the components of \mathbf{v} are generated by linear operations on these time functions, \mathbf{v} has a multivariate Gaussian distribution

$$p(\mathbf{v}|H_i) = \frac{1}{\det(\pi K_i)} \cdot \exp(-\mathbf{v}^* K_i^{-1} \mathbf{v}) \quad i = 0, 1 \quad (\text{A-10})$$

where

$$K_i = E\{\mathbf{v}\mathbf{v}^*|H_i\} \quad i = 0, 1 \quad (\text{A-11})$$

and \mathbf{v}^* denotes the conjugate transpose of \mathbf{v} . To obtain $\psi_0(s)$, one must substitute (A-10) into (A-8) and carry out the indicated algebraic operations. For observation time T large compared to the correlation time (inverse bandwidth) of signal and noise (i.e., $WT/2\pi \gg 1$), the Fourier coefficients (at each

receiver output) associated with different frequencies are statistically uncorrelated. In that case, the required computations become relatively easy. Details are contained in [9, Appendix A]. The result is

$$\psi_0(s) = \prod_k [1 + 4s(1-s) \Gamma(\omega_k, x)]^{-1} \quad (\text{A-12})$$

where

$$\omega_k = 2\pi k/T \quad (\text{A-13})$$

and

$$\Gamma(\omega_k, x) = \text{SNR}(\omega_k) \sin^2 \omega_k x/2. \quad (\text{A-14})$$

The index k varies over all components in the signal frequency band. Following very similar considerations for $\psi_1(s)$, one obtains

$$\psi_1(s) = \prod_k [1 - 4s(1+s) \Gamma(\omega_k, x)]^{-1}. \quad (\text{A-15})$$

Note that $\psi_0(s)$ and $\psi_1(s)$ depend only on x so that $P_e(a, a+x) = P_e(x)$. One must now substitute (A-12) and (A-15) into (A-6) and carry out the indicated integration. It can be easily shown that all the poles (singular points) of $\psi_0(s)$ are located on the real axis outside the interval $[0, 1]$, and all the poles of $\psi_1(s)$ are located on the real axis outside the interval $[-1, 0]$. Hence, the first integral in (A-6) can be evaluated for any value of c_0 in the open interval $(0, 1)$ without affecting the desired result. Similarly, the second integral in (A-6) can be evaluated for any value of c_1 in $(-1, 0)$. We shall find it most convenient to choose $c_0 = \frac{1}{2}$, $c_1 = -\frac{1}{2}$. We shall further make the change of variables $s = \frac{1}{2} + jy$ in the first integral and $s = -\frac{1}{2} + jy$ in the second integral. In this setting, one obtains

$$\begin{aligned} P_e(x) &= \frac{1}{2} \frac{1}{2\pi} \int_{-\infty}^\infty \frac{1}{\frac{1}{2} + jy} \left\{ \prod_k \left[1 + 4 \left(\frac{1}{2} + jy \right) \left(\frac{1}{2} - jy \right) \right. \right. \\ &\quad \left. \left. \cdot \Gamma(\omega_k, x) \right]^{-1} \right\} dy \\ &\quad - \frac{1}{2} \frac{1}{2\pi} \int_{-\infty}^\infty \frac{1}{-\frac{1}{2} + jy} \left\{ \prod_k \left[1 + 4 \left(\frac{1}{2} + jy \right) \left(\frac{1}{2} - jy \right) \right. \right. \\ &\quad \left. \left. \cdot \Gamma(\omega_k, x) \right]^{-1} \right\} dy \\ &= \frac{1}{\pi} \int_{-\infty}^\infty \left\{ \prod_k [1 + 1 + 4y^2] \Gamma(\omega_k, x) \right\}^{-1} \frac{dy}{1 + 4y^2} \\ &= \frac{2}{\pi} \left\{ \prod_k [1 + \Gamma(\omega_k, x)]^{-1} \right\} \\ &\quad \cdot \int_0^\infty \left\{ \prod_k \left[1 + \frac{\Gamma(\omega_k, x)}{1 + \Gamma(\omega_k, x)} 4y^2 \right]^{-1} \right\} \frac{dy}{1 + 4y^2}. \end{aligned} \quad (\text{A-16})$$

This is an exact expression for $P_e(x)$. To generate a lower bound on $P_e(x)$ we shall use the inequality $(1+x)^{-1} \geq e^{-x}$ whenever $x \geq 0$. Thus,

$$\left[1 + \frac{\Gamma(\omega_k, x)}{1 + \Gamma(\omega_k, x)} 4y^2\right]^{-1} \geq \exp \left\{ -\frac{\Gamma(\omega_k, x)}{1 + \Gamma(\omega_k, x)} 4y^2 \right\}. \quad (\text{A-17})$$

Substituting (A-17) into (A-16), one obtains

$$\begin{aligned} P_e(x) &\geq \left\{ \prod_k [1 + \Gamma(\omega_k, x)]^{-1} \right\} \frac{2}{\pi} \int_0^\infty \\ &\quad \cdot \exp \left\{ -4y^2 \sum_k \frac{\Gamma(\omega_k, x)}{1 + \Gamma(\omega_k, x)} \right\} \frac{dy}{1 + 4y^2} \\ &= e^{a(x)} \frac{2}{\pi} \int_0^\infty e^{-4y^2 b(x)} \frac{dy}{1 + 4y^2} \end{aligned} \quad (\text{A-18})$$

where we defined

$$a(x) = -\sum_k \ln [1 + \Gamma(\omega_k, x)] \quad (\text{A-19})$$

$$b(x) = \sum_k \frac{\Gamma(\omega_k, x)}{1 + \Gamma(\omega_k, x)}. \quad (\text{A-20})$$

The integral in (A-18) can be evaluated analytically using [12, p. 338, formula 3.466-1]. The result is given by

$$P_e(x) \geq e^{a(x) + b(x)} \phi(\sqrt{2b(x)}), \quad (\text{A-21})$$

which is the desired result. Substituting (A-14) into (A-19) and (A-20), one obtains

$$\begin{aligned} a(x) &= -\sum_k \ln [1 + \text{SNR}(\omega_k) \cdot \sin^2 \omega_k x/2] \\ &= -\frac{T}{2\pi} \sum_k \ln [1 + \text{SNR}(\omega_k) \cdot \sin^2 \omega_k x/2] \cdot \Delta\omega \end{aligned} \quad (\text{A-22})$$

$$\begin{aligned} b(x) &= \sum_k \frac{\text{SNR}(\omega_k) \cdot \sin^2 \omega_k x/2}{1 + \text{SNR}(\omega_k) \cdot \sin^2 \omega_k x/2} \\ &= \frac{T}{2\pi} \sum_k \frac{\text{SNR}(\omega_k) \cdot \sin^2 \omega_k x/2}{1 + \text{SNR}(\omega_k) \cdot \sin^2 \omega_k x/2} \cdot \Delta\omega \end{aligned} \quad (\text{A-23})$$

where we define $\Delta\omega = 2\pi/T$. For large WT product and smoothly varying signal and noise spectra, the function $\text{SNR}(\omega) \sin^2 \omega x/2$ changes only insignificantly over the frequency increment of $\Delta\omega$, so that the sums in (A-22) and (A-23) can be converted into the integrals given by (5) and (6), respectively.

Equation (A-21) can further be used to generate weaker lower bounds on $P_e(x)$, which will become useful in the proceeding analysis. We shall start from (A-19) and (A-20). Since

$$\frac{\Gamma(\omega_k, x)}{1 + \Gamma(\omega_k, x)} \leq \Gamma(\omega_k, x) \quad (\text{A-24})$$

and since

$$\ln [1 + \Gamma(\omega_k, x)] - \frac{\Gamma(\omega_k, x)}{1 + \Gamma(\omega_k, x)} \leq \frac{1}{2} \Gamma^2(\omega_k, x), \quad (\text{A-25})$$

it immediately follows that

$$2b(x) \leq 2 \sum_k \Gamma(\omega_k, x) \quad (\text{A-26})$$

and

$$a(x) + b(x) \geq -\frac{1}{2} \sum_k \Gamma^2(\omega_k, x) \quad (\text{A-27})$$

where $2b(x)$ and $[a(x) + b(x)]$ are the terms appearing in (A-21). Replacing the first term by its upper bound, and the second term by its lower bound, $P_e(x)$ can further be bounded by

$$P_e(x) \geq e^{-d(x)} \phi(\sqrt{c(x)}) \quad (\text{A-28})$$

where $c(x)$ and $d(x)$ are given by

$$\begin{aligned} c(x) &= 2 \sum_k \Gamma(\omega_k, x) = \frac{T}{\pi} \sum_k \text{SNR}(\omega_k) \sin^2(\omega_k x/2) \Delta\omega \\ &\xrightarrow{WT/2\pi \gg 1} \frac{T}{\pi} \int_0^\infty \text{SNR}(\omega) \cdot \sin^2(\omega x/2) d\omega \end{aligned} \quad (\text{A-29})$$

$$\begin{aligned} d(x) &= \frac{1}{2} \sum_k \Gamma^2(\omega_k, x) \\ &= \frac{T}{4\pi} \sum_k [\text{SNR}(\omega_k) \cdot \sin^2(\omega_k x/2)]^2 \Delta\omega \\ &\xrightarrow{WT/2\pi \gg 1} \frac{T}{4\pi} \int_0^\infty [\text{SNR}(\omega) \cdot \sin^2 \omega x/2]^2 d\omega. \end{aligned} \quad (\text{A-30})$$

Using the inequality $\sin^2(\omega x/2) \leq (\omega x/2)^2$, $c(x)$ and $d(x)$ can further be bounded by

$$c(x) \leq c^2 x^2 \quad (\text{A-31})$$

$$d(x) \leq d^4 x^4 \quad (\text{A-32})$$

where

$$c^2 = \frac{T}{4\pi} \int_0^\infty \omega^2 \text{SNR}(\omega) d\omega \quad (\text{A-33})$$

and

$$d^4 = \frac{T}{64\pi} \int_0^\infty [\omega^2 \text{SNR}(\omega)]^2 d\omega. \quad (\text{A-34})$$

Substituting $c(x)$ and $d(x)$ by their upper bounds, one immediately obtains

$$P_e(x) \geq e^{-d^4 x^4} \phi(cx). \quad (\text{A-35})$$

We note, in passing, that the lower bound given by (A-35) is useful only for small x where the inequalities in (A-31) and (A-32) are tight.

APPENDIX B

ANALYSIS OF THE MODIFIED ZZLB FOR BASEBAND SIGNALS

The modified ZZLB is given by (3), and is rewritten here for reference:

$$\bar{\epsilon}^2 \geq \frac{1}{D} \int_0^D x G[(D-x)P_e(x)] dx. \quad (\text{B-1})$$

The function $G[(D-x)P_e(x)]$ assumes a simple form if $P_e(x)$ contains several well-defined peaks. This is illustrated in Fig. 12 for a typical baseband case. Thus, if x_0, x_1, x_2, \dots are the local maxima of $P_e(x)$, then at each segment $[x_{n-1}, x_n]$ the function $G[(D-x)P_e(x)]$ is closely bounded by

$$G[(D-x)P_e(x)] \geq (D-x_n)P_e(x_n) \quad x_{n-1} \leq x \leq x_n. \quad (\text{B-2})$$

Note that since $G[(D-x)P_e(x)]$ is a nonincreasing function of x , (B-2) holds for arbitrary set of x_n 's. We further note that the local maxima of $P_e(x)$ are, in fact, the local maxima (ambiguity points) of the cross-correlation function. These occur, approximately, at (see Fig. 2)

$$x_n = (2\pi/W)n \quad n = 0, 1, 2, \dots \quad (\text{B-3})$$

$P_e(x_n)$, required for the computation of (B-2), is closely approximated using the expression in (4). Following the derivation in Appendix A, that expression is shown to be a lower bound. Thus,

$$P_e(x_n) \geq e^{a(x_n)+b(x_n)} \phi(\sqrt{2b(x_n)}) \quad (\text{B-4})$$

where $a(x_n)$ and $b(x_n)$ are obtained by substituting $x = x_n$ into (12) and (13), respectively. One obtains

$$\begin{aligned} a(x_n) &= -\frac{T}{2\pi} \int_0^{W/2} \ln(1 + \text{SNR} \cdot \sin^2 \omega x_n/2) d\omega \\ &= -\frac{WT}{2\pi} \frac{1}{Wx_n/2} \int_0^{Wx_n/4} \ln(1 + \text{SNR} \sin^2 \Omega) d\Omega \end{aligned} \quad (\text{B-5})$$

and

$$\begin{aligned} b(x_n) &= \frac{T}{2\pi} \int_0^{W/2} \frac{\text{SNR} \cdot \sin^2 \omega x_n/2}{1 + \text{SNR} \cdot \sin^2 \omega x_n/2} d\omega \\ &= \frac{WT}{2\pi} \frac{1}{Wx_n/2} \int_0^{Wx_n/4} \frac{\text{SNR} \cdot \sin^2 \Omega}{1 + \text{SNR} \cdot \sin^2 \Omega} d\Omega \end{aligned} \quad (\text{B-6})$$

where $Wx_n/4 = n\pi/2$. Since the integrands in (B-5) and (B-6) are even and periodic functions of Ω with a period of π , and

since we are integrating over $[0, n\pi/2]$, these equations become independent of n , i.e., $a(x_n) = a$ and $b(x_n) = b$, where

$$\begin{aligned} a &= -\frac{WT}{2\pi} \cdot \frac{1}{\pi} \int_0^{\pi/2} \ln(1 + \text{SNR} \sin^2 \Omega) d\Omega \\ &= -\frac{WT}{2\pi} \ln \frac{1 + \sqrt{1 + \text{SNR}}}{2} \end{aligned} \quad (\text{B-7})$$

$$\begin{aligned} b &= \frac{WT}{2\pi} \frac{1}{\pi} \int_0^{\pi/2} \frac{\text{SNR} \cdot \sin^2 \Omega}{1 + \text{SNR} \cdot \sin^2 \Omega} d\Omega \\ &= \frac{WT}{4\pi} \frac{\sqrt{1 + \text{SNR}} - 1}{\sqrt{1 + \text{SNR}}}. \end{aligned} \quad (\text{B-8})$$

The integral appearing in (B-7) can be found in [12, p. 594, formula 4.399]. The integral appearing in (B-8) can be modified to a form found in [12, p. 152, formula 2.562]. Thus,

$$P_e(x_n) \geq e^{a+b} \phi(\sqrt{2b}). \quad (\text{B-9})$$

Substituting (B-3) and (B-9) into (B-2), one obtains

$$\begin{aligned} G[(D-x)P_e(x)] &\geq (D-x_n) e^{a+b} \phi(\sqrt{2b}) \\ x_n - 2\pi/W &\leq x \leq x_n. \end{aligned} \quad (\text{B-10})$$

Since $D - x_n \geq D - 2\pi/W - x$ for all $x \in [x_n - 2\pi/W, x_n]$, it immediately follows that

$$G[(D-x)P_e(x)] \geq \begin{cases} (D - 2\pi/W - x) e^{a+b} \phi(\sqrt{2b}) & 0 \leq x \leq D - 2\pi/W \\ 0 & D - 2\pi/W \leq x \leq D. \end{cases} \quad (\text{B-11})$$

The first line in (B-11) is illustrated by the dashed line in Fig. 12. The second line in (B-11) indicates that zero is a better bound. For $WD/2\pi \gg 1$, the lower bound presented by (B-11) is very tight except for values of x in the vicinity of $x = 0$ where $P_e(x)$ changes rapidly.

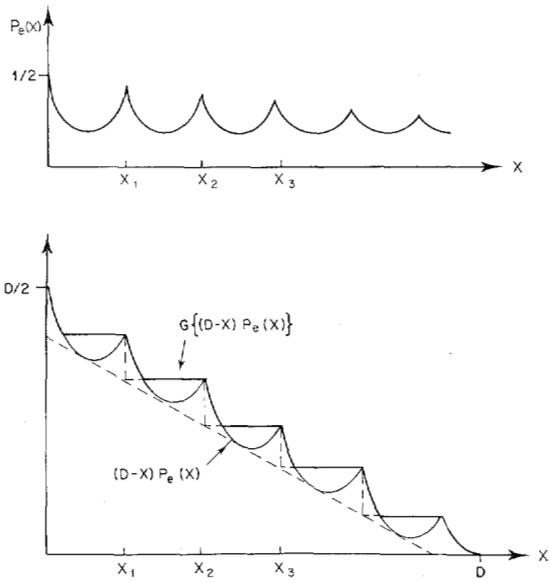
To take this effect into account, we observe that for small x , $P_e(x)$ is closely bounded using (A-35). In that region, therefore, $G[(D-x)P_e(x)]$ is closely bounded by

$$\begin{aligned} G[(D-x)P_e(x)] &\geq G[(D-x)e^{-d^4 x^4} \phi(cx)] \\ &= (D-x) e^{-d^4 x^4} \phi(cx) \end{aligned} \quad (\text{B-12})$$

where, in the transition from the first version of (B-12) to its second version, we observe that $G[f(x)] = f(x)$ whenever $f(x)$ is a nonincreasing function of x . The parameters c and d are obtained by substituting (10) into (A-33) and (A-34), respectively. One obtains

$$c^2 = \frac{T}{4\pi} \int_0^{W/2} \omega^2 \text{SNR} d\omega = \frac{W^3 T \text{SNR}}{96\pi} \quad (\text{B-13})$$

$$d^4 = \frac{T}{64\pi} \int_0^{W/2} [\omega^2 \text{SNR}]^2 d\omega = \frac{W^5 T \text{SNR}^2}{5 \cdot 2^{11} \cdot \pi}. \quad (\text{B-14})$$

Fig. 12. $P_e(x)$ and $G[(D-x)P_e(x)]$ for typical baseband case.

For future manipulations we note that

$$(c/d)^4 = \frac{20}{9} (WT/2\pi). \quad (\text{B-15})$$

Combining (B-11) and (B-12), $G[(D-x)P_e(x)]$ is tightly bounded by

$$G[(D-x)P_e(x)] \geq \begin{cases} (D-x)e^{-d^4x^4}\phi(cx) & 0 \leq x \leq z \\ (D-2\pi/W-x)e^{a+b}\phi(\sqrt{2b}) & z < x \leq D-2\pi/W \\ 0 & D-2\pi/W < x \leq D \end{cases} \quad (\text{B-16})$$

where z is defined by

$$cz = \sqrt{2b}. \quad (\text{B-17})$$

Note that z is approximately the point at which the first and second lines in (B-16) intersect. Substituting (B-16) into (B-1) one obtains the following lower bound:

$$\begin{aligned} \bar{\epsilon}^2 \geq & \frac{1}{D} \int_0^z x(D-x)e^{-d^4x^4}\phi(cx) dx \\ & + \left[\frac{1}{D} \int_z^{D-2\pi/W} x(D-2\pi/W-x) dx \right] e^{a+b}\phi(\sqrt{2b}). \end{aligned} \quad (\text{B-18})$$

Carrying out some straightforward algebra manipulations, it can easily be shown that $z < 2\pi/W$. Since we are assuming that $2\pi/W \ll D$, the first term on the right-hand side of (B-18) is closely approximated by

$$\frac{1}{D} \int_0^z x(D-x)e^{-d^4x^4}\phi(cx) dx \approx \int_0^z xe^{-d^4x^4}\phi(cx) dx$$

$$\begin{aligned} &= \frac{1}{c^2} \int_0^{cz} x \exp \left\{ -\frac{x^4}{(c/d)^4} \right\} \phi(x) dx \\ &= \frac{1}{c^2} \int_0^{\sqrt{2b}} x \cdot \exp \left\{ -\frac{9x^4}{20(WT/2\pi)} \right\} \phi(x) dx \end{aligned} \quad (\text{B-19})$$

where, in the transition from the second version of (B-19) to its third version, we have substituted (B-15) and (B-17). Similarly, the integral appearing in the second term of (B-18) is closely approximated by

$$\frac{1}{D} \int_z^{D-2\pi/W} x(D-2\pi/W-x) dx \approx D^2/6. \quad (\text{B-20})$$

Substituting (B-19) and (B-20) into (B-18), one obtains

$$\begin{aligned} \bar{\epsilon}^2 \geq & \frac{1}{c^2} \int_0^{\sqrt{2b}} x \cdot \exp \left\{ -\frac{9x^4}{20(WT/2\pi)} \right\} \phi(x) dx \\ & + \frac{D^2}{6} e^{a+b}\phi(\sqrt{2b}). \end{aligned} \quad (\text{B-21})$$

Numerical integration indicates that (B-21) is an excellent approximation to the exact result (B-1). The lower bound presented by (B-21) exhibits two distinct asymptotes: as $\text{SNR} \rightarrow 0$, the variables a , b , and c approach zero. In that limit, the second term in (B-21) becomes the dominant term and the lower bound approaches

$$\bar{\epsilon}^2 \approx D^2/12. \quad (\text{B-22})$$

As $\text{SNR} \rightarrow \infty$, $a+b \rightarrow -\infty$ and $b \rightarrow WT/4\pi$. In that limit, the first term in (B-21) becomes the dominant term in the sum and the lower bound approaches

$$\begin{aligned} \bar{\epsilon}^2 \geq & \frac{1}{c^2} \int_0^{\sqrt{WT/2\pi}} x \cdot \exp \left\{ -\frac{9x^4}{20(WT/2\pi)} \right\} \phi(x) dx \\ & \xrightarrow{WT/2\pi \gg 1} \frac{1}{c^2} \int_0^\infty x \phi(x) dx = \frac{1}{4c^2} \\ & = \frac{12}{W^2} \cdot \frac{1}{(WT/2\pi) \text{SNR}}. \end{aligned} \quad (\text{B-23})$$

One immediately identifies (B-22) with the first line of (14), and (B-23) with its third line.

The transition from the $D^2/12$ asymptote to the $1/4c^2$ asymptote essentially starts when

$$e^{a+b}\phi(\sqrt{2b}) = \frac{1}{4} \quad (\text{B-24})$$

and is essentially completed when

$$\frac{D^2}{6} e^{a+b}\phi(\sqrt{2b}) = 1/4c^2 \quad (\text{B-25})$$

where, in the transition region (the so-called threshold region), the lower bound varies essentially as $\phi(\sqrt{2b})$. One must now substitute (B-7), (B-8), and (B-13) into (B-24) and (B-25), and solve these equations with respect to SNR in order to obtain the corresponding 3 dB points. Suppose, for the moment, that

these solutions are obtained at $\text{SNR} \ll 1$. In that case, (B-7) and (B-8) can be approximated, without incurring any significant errors, by

$$a \approx -\frac{WT}{2\pi} \ln(1 + \text{SNR}/4) \approx -\frac{WT}{2\pi} \cdot \frac{\text{SNR}}{4} \quad (\text{B-26})$$

$$b \approx \frac{WT}{4\pi} \cdot \frac{\text{SNR}}{2}. \quad (\text{B-27})$$

With these approximations, (B-24) and (B-25) assume the simplified forms

$$\phi(\sqrt{R/2}) = \frac{1}{4} \quad (\text{B-28})$$

and

$$(R/2)\phi(\sqrt{R/2}) = (6/WD)^2 \quad (\text{B-29})$$

where R is the postintegration SNR defined by

$$R = (WT/2\pi) \text{SNR}. \quad (\text{B-30})$$

Denoting by $R = \alpha$ the solution to (B-28), and substituting $2[\phi^{-1}(\frac{1}{4})]^2 = 0.92$, one immediately obtains (15). Denoting by $R = \beta$ the solution to (B-29), one immediately obtains (16). We further observe that in terms of SNR, the solution to (B-28) reads $\text{SNR} = \alpha/(WT/2\pi)$, and the solution to (B-29) reads $\text{SNR} = \beta/(WT/2\pi)$. Thus, for $WT/2\pi \gg 1$, the simplifying approximations made in (B-26) and (B-27) may affect these results only insignificantly.

APPENDIX C

ANALYSIS OF THE MODIFIED ZZLB FOR BANDPASS SIGNALS

The modified ZZLB is given by (3) and is rewritten here for reference:

$$\bar{\epsilon}^2 \geq \frac{1}{D} \int_0^D x G[(D-x)P_e(x)] dx. \quad (\text{C-1})$$

For values of x in the vicinity of $x=0$, the function $G[(D-x)P_e(x)]$ is closely bounded using (B-12) where the parameters c and d are obtained by substituting (19) into (A-33) and (A-34), respectively. Assuming that $\omega_0/W \gg 1$ (so that one can ignore terms on the order of $(W/\omega_0)^2$ relative to 1), c^2 and d^4 are given, respectively, by

$$c^2 = \frac{WT}{4\pi} \omega_0^2 \text{SNR} \quad (\text{C-2})$$

$$d^4 = \frac{WT}{64\pi} \omega_0^4 \text{SNR}^2. \quad (\text{C-3})$$

For future manipulations, we note that

$$(c/d)^4 = 8(WT/2\pi). \quad (\text{C-4})$$

For values of x away from $x=0$, a tighter lower bound on $G[(D-x)P_e(x)]$ can be generated from the local maxima of $P_e(x)$. This is illustrated in Fig. 12 for a typical baseband case. In the bandpass case, however, $P_e(x)$ has two sets of local maxima. One set, $x_n = (2\pi/W)n$, $n=1, 2, \dots$, is associated with the ambiguities in the envelope of the cross-correlation

function, and the other set, $\tilde{x}_n = (2\pi/\omega_0)n$, is associated with the ambiguities in the phase of the cross-correlation function.

We shall assume, without any significant loss in generality, that $\omega_0/W = k$ is an integer. In that case, using the set $x_n = (2\pi/W)n$ and following the same considerations outlined in Appendix B, $G[(D-x)P_e(x)]$ is bounded using (B-11), where a and b are given by

$$a = -\frac{WT}{\pi} \ln \frac{1 + \sqrt{1 + \text{SNR}}}{2} \quad (\text{C-5})$$

$$b = \frac{WT}{2\pi} \frac{\sqrt{1 + \text{SNR}} - 1}{\sqrt{1 + \text{SNR}}}. \quad (\text{C-6})$$

Note that there is a factor of 2 difference between (C-5) and (B-7), and between (C-6) and (B-8).

We shall now use the set $\tilde{x}_n = (2\pi/\omega_0)n$ to generate another lower bound on $G[(D-x)P_e(x)]$ using similar considerations. Making use of (A-28), $P_e(\tilde{x}_n)$ is bounded by

$$P_e(\tilde{x}_n) \geq e^{-d(\tilde{x}_n)} \phi(\sqrt{c(\tilde{x}_n)}) \quad (\text{C-7})$$

where $c(\tilde{x}_n)$ and $d(\tilde{x}_n)$ are obtained by substituting (19) into (A-29) and (A-30), and calculating these functions for $x = \tilde{x}_n$. Following some straightforward algebra manipulations, one obtains

$$c(\tilde{x}_n) = \frac{WT}{2\pi} \frac{1}{W\tilde{x}_n/2} \int_{-W\tilde{x}_n/4}^{W\tilde{x}_n/4} \text{SNR} \cdot \sin^2 \Omega d\Omega \quad (\text{C-8})$$

$$d(\tilde{x}_n) = \frac{WT}{4\pi} \frac{1}{W\tilde{x}_n/2} \int_{-W\tilde{x}_n/4}^{W\tilde{x}_n/4} [\text{SNR} \cdot \sin^2 \Omega]^2 d\Omega. \quad (\text{C-9})$$

Using the inequality $\sin^2 \Omega \leq \Omega$, $c(\tilde{x}_n)$ and $d(\tilde{x}_n)$ can be bounded by

$$c(\tilde{x}_n) \leq \tilde{c}^2 \tilde{x}_n^2 \quad (\text{C-10})$$

$$d(\tilde{x}_n) \leq \tilde{d}^4 \tilde{x}_n^4 \quad (\text{C-11})$$

where

$$\tilde{c}^2 = \frac{W^3 T \text{SNR}}{48\pi} \quad (\text{C-12})$$

$$\tilde{d}^4 = \frac{W^5 T \text{SNR}^2}{5 \cdot 2^{10} \cdot \pi}. \quad (\text{C-13})$$

For future manipulations, we note that

$$(\tilde{c}/\tilde{d})^4 = \frac{40}{9} (WT/2\pi). \quad (\text{C-14})$$

Substituting $c(\tilde{x}_n)$ and $d(\tilde{x}_n)$ by their upper bounds, one obtains

$$P_e(\tilde{x}_n) \geq e^{-\tilde{d}^4 \tilde{x}_n^4} \phi(\tilde{c} \tilde{x}_n). \quad (\text{C-15})$$

Now, since

$$G[(D-x)P_e(x)] \geq (D-\tilde{x}_n)P_e(\tilde{x}_n) \quad \tilde{x}_n - 2\pi/\omega_0 \leq x \leq \tilde{x}_n, \quad (\text{C-16})$$

and since the right-hand side of (C-15) is a monotonically decreasing function, it immediately follows that

$$G[(D-x)P_e(x)] \geq (D-2\pi/\omega_0-x)e^{-\tilde{d}^4(x+2\pi/\omega_0)^4} \cdot \phi[\tilde{c}(x+2\pi/\omega_0)]. \quad (C-17)$$

Combining (B-12), (C-17), and (B-11) (in the given order), $G[(D-x)P_e(x)]$ is tightly bounded by

$$G[(D-x)P_e(x)] \geq \begin{cases} (D-x)e^{-\tilde{d}^4 x^4} \phi(cx) & 0 \leq x < z_1 \\ (D-2\pi/\omega_0-x)e^{-\tilde{d}^4(x+2\pi/\omega_0)^4} \phi[\tilde{c}(x+2\pi/\omega_0)] & z_1 \leq x < z_2 \\ (D-2\pi/W-x)e^{a+b} \phi(\sqrt{2b}) & z_2 \leq x < D-2\pi/n \\ 0 & D-2\pi/W \leq x \leq D \end{cases} \quad (C-18)$$

where z_1 and z_2 are defined by

$$cz_1 = \tilde{c}(z_1 + 2\pi/\omega_0) \quad (C-19)$$

$$\tilde{c}(z_2 + 2\pi/\omega_0) = \sqrt{2b}. \quad (C-20)$$

Note that z_1 is approximately the point at which the first and second lines in (C-18) intersect, and z_2 is approximately the point at which the second and third lines intersect. Substituting (C-18) into (C-1), one obtains the following lower bound:

$$\begin{aligned} \bar{\epsilon}^2 &\geq \frac{1}{D} \int_0^{z_1} x(D-x)e^{-\tilde{d}^4 x^4} \phi(cx) dx \\ &+ \frac{1}{D} \int_{z_1}^{z_2} x(D-2\pi/\omega_0-x)e^{-\tilde{d}^4(x+2\pi/\omega_0)^4} \\ &\cdot \phi[\tilde{c}(x+2\pi/\omega_0)] dx \\ &+ \left[\frac{1}{D} \int_{z_2}^{D-2\pi/W} x(D-2\pi/W-x) dx \right] e^{a+b} \phi(\sqrt{2b}). \end{aligned} \quad (C-21)$$

Following some straightforward algebra manipulations, it can easily be shown that $z_1 \ll 2\pi/\omega_0$, and that $z_2 < 2\pi/W$. Since we are assuming that $2\pi/W \ll D$, the lower bound can be approximated, without incurring any significant errors, by

$$\begin{aligned} \bar{\epsilon}^2 &\geq \sim \int_0^{z_1} x e^{-\tilde{d}^4 x^4} \phi(cx) dx \\ &+ \int_{z_1}^{z_2} x e^{-\tilde{d}^4(x+2\pi/\omega_0)^4} \phi[\tilde{c}(x+2\pi/\omega_0)] dx \\ &+ \frac{D^2}{6} e^{a+b} \phi(\sqrt{2b}) \\ &= \frac{1}{c^2} \int_0^{cz_1} x \cdot \exp \left\{ -\frac{x^4}{(c/d)^4} \right\} \phi(x) dx \end{aligned}$$

$$\begin{aligned} &+ \frac{1}{\tilde{c}^2} \int_{\tilde{c}(z_1+2\pi/\omega_0)}^{\tilde{c}(z_2+2\pi/\omega_0)} (x - \tilde{c} \cdot 2\pi/\omega_0) \\ &\cdot \exp \left\{ -\frac{x^4}{(\tilde{c}/d)^4} \right\} \phi(x) dx + \frac{D^2}{6} e^{a+b} \phi(\sqrt{2b}) \\ &= \frac{1}{c^2} \int_0^{\tilde{c}(z_1+2\pi/\omega_0)} x \cdot \exp \left\{ -\frac{x^4}{8(WT/2\pi)} \right\} \phi(x) dx \\ &+ \frac{1}{\tilde{c}^2} \int_{\tilde{c}(z_1+2\pi/\omega_0)}^{\sqrt{2b}} (x - \tilde{c}2\pi/\omega_0) \\ &\cdot \exp \left\{ -\frac{9x^4}{40(WT/2\pi)} \right\} \phi(x) dx + \frac{D^2}{6} e^{a+b} \phi(\sqrt{2b}) \\ &\approx \frac{1}{c^2} \int_0^{\tilde{c}2\pi/\omega_0} x \cdot \exp \left\{ -\frac{x^4}{8(WT/2\pi)} \right\} \phi(x) dx \\ &+ \frac{1}{\tilde{c}^2} \int_{\tilde{c}2\pi/\omega_0}^{\sqrt{2b}} (x - \tilde{c}2\pi/\omega_0) \\ &\cdot \exp \left\{ -\frac{9x^4}{40(WT/2\pi)} \right\} \phi(x) dx + \frac{D^2}{6} e^{a+b} \phi(\sqrt{2b}). \end{aligned} \quad (C-22)$$

where, in the transition from the second version of (C-22) to its third version, we have substituted (C-4), (C-14), (C-19), and (C-20).

Substituting (C-2), (C-12), (C-5), and (C-6) into (C-22), one can now generate MSE predictions for any prespecified SNR. We further note that the second and third terms in (C-22) contribute significantly to the sum only when $\text{SNR} \ll 1$. In that region, a and b can be approximated, without incurring any significant errors, by

$$a \approx -\frac{WT}{\pi} \cdot \frac{\text{SNR}}{4} \quad (C-23)$$

$$b \approx \frac{WT}{2\pi} \cdot \frac{\text{SNR}}{2}. \quad (C-24)$$

With these considerations, the lower bound assumes the form

$$\begin{aligned} \bar{\epsilon}^2 &\geq \frac{1}{(\omega_0^2/2)R} \int_0^{\sqrt{(\pi^2/6)(W/\omega_0)}\sqrt{R}} x \cdot \exp \left\{ -\frac{x^4}{8(WT/2\pi)} \right\} \\ &\cdot \phi(x) dx \\ &+ \frac{1}{(W^2/24)R} \int_{\sqrt{(\pi^2/6)(W/\omega_0)}\sqrt{R}}^{\sqrt{R}} x \\ &\cdot \exp \left\{ -\frac{9x^4}{40(WT/2\pi)} \right\} \phi(x) dx + \frac{D^2}{6} \phi(\sqrt{R}) \end{aligned} \quad (C-25)$$

where R is defined as the product of $WT/2\pi$ by SNR (the so-called postintegration SNR).

We shall now examine a few limiting cases. If $R \ll 1$, the third term on the right-hand side of (C-25) becomes the dominant term in the sum, and the lower bound approaches

$$\bar{\epsilon}^2 \geq \sim \frac{D^2}{6} \phi(\sqrt{R}) \rightarrow \frac{D^2}{12} \quad (C-26)$$

If $1 \ll R \ll (\omega_0/W)^2$, the second term becomes the dominant term in the sum, and the lower bound approaches

$$\begin{aligned} \bar{\epsilon}^2 &\geq \sim \frac{1}{(W^2/24)R} \int_{\sqrt{(\pi^2/6)(W/\omega_0)\sqrt{R}}}^{\sqrt{R}} x \\ &\quad \cdot \exp \left\{ -\frac{9x^4}{40(WT/2\pi)} \right\} \phi(x) dx \\ &\xrightarrow{(WT/2\pi) \gg 1} \frac{1}{(W^2/12)R} \phi \left(\sqrt{\frac{\pi^2}{6} \frac{W}{\omega_0} \sqrt{R}} \right) \\ &\approx \frac{1}{(W^2/6)R} \end{aligned} \quad (C-27)$$

Finally, if $R \gg (\omega_0/W)^2$, the first term in the sum becomes the dominant one, and the lower bound approaches

$$\begin{aligned} \bar{\epsilon}^2 &\geq \sim \frac{1}{(\omega_0^2/2)R} \int_0^{\sqrt{(\pi^2/6) \cdot (W/\omega_0)\sqrt{R}}} x \\ &\quad \cdot \exp \left\{ -\frac{x^4}{8(WT/2\pi)} \right\} \phi(x) dx \\ &\xrightarrow{WT/2\pi \gg 1} \frac{1}{2\omega_0^2 R} \left[1 - 2\phi \left(\sqrt{\frac{\pi^2}{6} \frac{W}{\omega_0} \sqrt{R}} \right) \right] \\ &\approx \frac{1}{2\omega_0^2 R} \end{aligned} \quad (C-28)$$

One immediately identifies (C-26), (C-27), and (C-28) with the first, third, and fifth lines of (22), respectively.

The transition from the first line of (22) to its third line essentially starts when

$$\phi(\sqrt{R}) = \frac{1}{4} \quad (C-29)$$

and is essentially completed when

$$\frac{D^2}{6} \phi(\sqrt{R}) = \frac{1}{(W^2/6)R}, \quad (C-30)$$

where, in the transition region, the lower bound varies essentially as $\phi(\sqrt{R})$. Denoting by $R = \gamma$ the solution to (C-29), and using the similarity between (C-29) and (B-28), one immediately obtains (26). Denoting by $R = \delta$ the solution to (C-30), and using the similarity between (C-30) and (B-29), one immediately obtains (27).

The transition from the third line of (22) to its fifth line essentially starts when

$$\phi \left(\sqrt{\frac{\pi^2}{6} \frac{W}{\omega_0} \sqrt{R}} \right) = \frac{1}{4} \quad (C-31)$$

and is essentially completed when

$$\frac{1}{(W^2/12)R} \phi \left(\sqrt{\frac{\pi^2}{6} \frac{W}{\omega_0} \sqrt{R}} \right) = \frac{1}{2\omega_0^2 R} \quad (C-32)$$

where, in the transition region, the lower bound varies essentially as $\phi(\sqrt{(\pi^2/6)W/\omega_0 \sqrt{R}})$. Denoting by $R = \mu$ and $R = \eta$

the solutions to (C-31) and (C-32), and following some straightforward algebra manipulations, one immediately obtains (24) and (25), respectively.

ACKNOWLEDGMENT

The authors would like to thank Prof. P. M. Schultheiss and Dr. J. P. Ianniello for their helpful comments and discussions throughout the course of study, and to the Word Processing Department at Tel-Aviv University for their patient and excellent secretarial assistance.

REFERENCES

- [1] V. H. MacDonald and P. M. Schultheiss, "Optimum passive bearing estimation in a spatially incoherent noise environment," *J. Acoust. Soc. Amer.*, vol. 46, pp. 37-43, 1969.
- [2] W. R. Hahn, "Optimum signal processing for passive sonar range and bearing estimation," *J. Acoust. Soc. Amer.*, vol. 58, no. 1, pp. 201-207, 1981.
- [3] G. C. Carter, "Time delay estimation for passive sonar signal processing," *IEEE Trans. Acoust., Speech, Signal Processing*, vol. ASSP-29, pp. 463-470, June 1981.
- [4] Y. T. Chan, R. V. Hattin, and J. B. Plant, "The least squares estimation of time delay and its use in signal detection," *IEEE Trans. Acoust., Speech, Signal Processing*, vol. ASSP-26, no. 3, pp. 217-222, 1978.
- [5] W. R. Hahn and S. A. Tretter, "Optimum processing for delay-vector estimation in passive signal arrays," *IEEE Trans. Inform. Theory*, vol. IT-19, no. 5, pp. 608-614, 1973.
- [6] B. V. Hamon and E. J. Hannan, "Spectral estimation of time delay for dispersive and nondispersive systems," *J. Appl. Statist.*, vol. 23, no. 2, pp. 134-142, 1974.
- [7] C. H. Knapp and G. C. Carter, "The generalized correlation method for estimation of time delay," *IEEE Trans. Acoust., Speech, Signal Processing*, vol. ASSP-24, no. 4, pp. 320-327, 1976.
- [8] A. J. Weiss and E. Weinstein, "Composite bound on the attainable mean-square error in passive time-delay estimation from ambiguity prone signal," *IEEE Trans. Inform. Theory*, vol. IT-28, pp. 977-979, Nov. 1982.
- [9] —, "Fundamental limitations in passive time delay estimation—Part I: Narrow-band systems," *IEEE Trans. Acoust., Speech, Signal Processing*, vol. ASSP-31, pp. 472-486, Apr. 1983.
- [10] J. P. Ianniello, E. Weinstein, and A. Weiss, "Comparison of the Ziv-Zakai lower bound on time delay estimation with correlator performance," in *Proc. IEEE Int. Conf. Acoust., Speech, Signal Processing (ICASSP'83)*, Apr. 1983.
- [11] S. K. Chow and P. M. Schultheiss, "Delay estimation using narrow-band processes," *IEEE Trans. Acoust., Speech, Signal Processing*, vol. ASSP-29, pp. 478-484, June 1981.
- [12] I. S. Gradshteyn and I. M. Ryzhik, *Tables of Integrals, Series and Products*. New York: Academic, 1980.

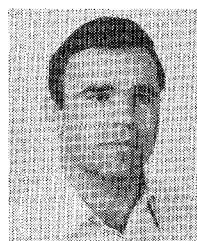


Ehud Weinstein (M'82) was born in Tel-Aviv, Israel, in May 1950. He received the B.Sc. degree in electrical engineering from the Technion-Israel Institute of Technology, Haifa, in 1975, and the M.Sc. and Ph.D. degrees from Yale University, New Haven, CT, in 1976 and 1978, respectively.

In 1978 he joined the Ocean Engineering Department, Woods Hole Oceanographic Institute, Woods Hole, MA, where he is currently an Associate Scientist. In 1980 he also joined the

Department of Electronic Systems, School of Engineering, Tel-Aviv University, where he is currently a Senior Lecturer. His research activities are in the areas of statistical detection and estimation, time delay estimation, and various signal processing problems in radar/sonar systems.

Dr. Weinstein was corecipient, with Anthony J. Weiss, of the IEEE Acoustics, Speech, and Signal Processing Society's 1983 Senior Award for the paper, "Fundamental limitations in passive time delay estimation—Part I: Narrow-band systems."



Anthony J. Weiss (S'84) was born in London, England, in March 1951. He received the B.Sc. degree (cum laude) from the Technion-Israel Institute of Technology, Haifa, in 1973, and the M.Sc. degree (magna cum laude) from Tel-Aviv University in 1982, both in electrical engineering.

From 1973 to 1983 he was involved in research and development of numerous projects in the areas of electromagnetic propagation, microwaves, tracking systems, command and

control, and direction finding. He is currently a consultant in the above areas. In 1984 he joined the Department of Electronic Systems, School of Engineering, Tel-Aviv University, where he is a research student towards the Ph.D. degree. His research activities are detection and estimation theory, signal processing, radar, sonar, and especially emitter localization and time delay estimation.

Mr. Weiss was corecipient, with Dr. Ehud Weinstein, of the IEEE Acoustics, Speech, and Signal Processing Society's 1983 Senior Award for the paper, "Fundamental limitations in passive time delay estimation—Part I: Narrow-band systems."

Correspondence

Weight Modulation Effects in the Adaptive Line Enhancer

Y. H. CHANG AND N. J. BERSHAD

Abstract—The steady-state behavior of the adaptive line enhancer is modeled by the sum of two filters, the Wiener weight filter and a weight misadjustment filter. The effects of randomly time-varying coefficients in the weight misadjustment filter are modeled so as to display line broadening of single frequency ALE inputs.

I. INTRODUCTION

In a recent paper [1], a steady-state model for computing the second-order output statistics of the adaptive line enhancer (ALE) was presented. The paper modeled the steady-state ALE as consisting of the sum of two linear fixed parameter filters operating upon the input data. The two filters were obtained by representing the converged ALE weights as the sum of the mean weight w^* plus a zero mean fluctuation part \tilde{w} . The mean weight w^* is the Wiener filter for the problem (i.e., the LMS adaptive algorithm converges, on the average, to the Wiener filter). The covariance of the fluctuations (weight misadjustment) was assumed proportional to μ , the algorithm adaptation parameter.

As stated in the paper, the steady-state impulse response of the ALE is a very slowly varying vector random process with mean w^* and fluctuation \tilde{w} . By assuming a sufficiently small value of μ , the weight vector was modeled as being constant over time intervals which are large relative to the length of the transversal filter.

The primary purpose of this note is to extend the results of that paper to larger values of μ where the effects of time-varying weight fluctuations are also included in the model. As expected,

Manuscript received October 13, 1983; revised February 20, 1984. This work is based in part on the Ph.D. dissertation of Y. H. Chang.

Y. H. Chang is with the Chung Shan Institute of Science and Technology, Taiwan.

N. J. Bershad is with the School of Engineering, University of California, Irvine, Irvine, CA 92717.

it is shown that the time-varying properties of the weights give rise to intermodulation products of the input and the filter weight fluctuations. The extended model gives rise to spectral broadening at the filter output. For a single frequency line component in the input (as is usually the case for application of the ALE), this effect could be a significant phenomenon that is not predicted by the previous model.

II. ANALYSIS

For purposes of analytic simplicity, we shall consider the complex model of the LMS algorithm and the resulting complex ALE. The analyses of the behavior of the real ALE yield very similar results [2], [3]. In order to compute the second-order output statistics of the ALE, it is first necessary to compute the second-order weight statistics over time.

A. Weight Statistics Over Time

The vector difference equation for the complex LMS algorithm [4] is given by

$$W(n+1) = [I - \mu X(n) X^\dagger(n)] W(n) + \mu d^*(n) X(n) \quad (1)$$

where

$W(n)$ = vector of weights on the n th iteration of the algorithm

$X(n)$ = data vector at time n

$d(n)$ = desired scalar signal at time n

μ = algorithm adaptation constant

\dagger = conjugate transpose.

Equation (1) has an explicit matrix solution which can be derived iteratively:

$$W(n) = \begin{cases} [I - \mu X(0) X^\dagger(0)] W(0) + \mu d^*(0) X(0), & n = 1 \\ \prod_{k=0}^{n-1} [I - \mu X(k) X^\dagger(k)] W(0) \\ + \mu \sum_{k=0}^{n-2} \prod_{m=k+1}^{n-1} [I - \mu X(m) X^\dagger(m)] \\ \cdot d^*(k) X(k) + \mu d^*(n-1) X(n-1), & n \geq 2. \end{cases} \quad (2)$$